Rosa-Ramírez, HDL.; Aldás-Carrasco, MF.; Ferri, J.; López-Martínez, J.; Samper, M. (2020). Modification of poly (lactic acid) through the incorporation of gum rosin and gum rosin derivative: Mechanical performance and hydrophobicity. Journal of Applied Polymer Science. 137(44):1-15. https://doi.org/10.1002/app.49346

Modification of poly (lactic acid) through the incorporation of gum rosin and gum rosin derivative: mechanical performance and hydrophobicity

H. De La Rosa-Ramírez [(1)*], M. Aldas [(1, 2)], J.M. Ferri [(1)], J. Lopez-Martínez [(1)], M.D. Samper [(1)*]

(1) Instituto de Tecnología de Materiales (ITM), Universitat Politècnica de València (UPV), Plaza Ferrándiz y Carbonell 1, 03801 Alcoy, Alicante, Spain

(2) Departamento de Ciencia de Alimentos y Biotecnología, Facultad de Ingeniería Química y Agroindustria, Escuela Politécnica Nacional, 170517 Quito, Ecuador

*Corresponding author: Harrison de la Rosa Ramírez, María Dolores Samper Madrigal
E-mail: harrison.dr@hotmail.com, hardela@epsa.upv.es, masammad@upvnet.upv.es

Postal address:
Laboratorio C1L2
Universitat Politècnica de València
Instituto Tecnológico de Materiales. Campus Alcoy
Plaza Ferrándiz y Carbonell nº 1,
03801 Alcoy (Alicante), Spain

Abstract

The modification of PLA by melt compound with gum rosin (GR) and pentaerythritol ester of GR (PEGR), was investigated by studying the mechanical and thermal performance, blends morphology, wettability, and water absorption. Standard testing specimens for characterization were made at a variate resin content of 5, 10 and 15 part per hundred resin (phr) and manufactured by injection molding. It was found that GR and PEGR had a lubricating effect in PLA polymeric chains, resulting in a remarkable increase of 790 and 193 % in melt flow index with only 5 phr GR and PEGR contents, respectively. A significant change in more than 10° of increasing water contact angle was observed for PLA with 15 phr PEGR. Thermo-gravimetric analysis reveals that PEGR led to delayed PLA degradation/decomposition process to higher temperature, increasing the onset temperature ($T_{5\%}$) in more than 7 °C for PLA with 15 phr PEGR.

Keywords: gum rosin, colophony, poly (lactic acid), pentaerythritol ester of gum rosin.

1 Introduction

It is a fact that conventional polymers of petrochemical origin and their different formulations continue to exceed in common use and industrial applications (domestic plastic products, packaging industry, agriculture consumption, etc.) the eco-friendly polymers that have been developed in the last decades. The reduced number of application fields of those eco-friendly polymers is mainly due to their limited properties, processability and its high prices compared with conventional polymers. However, there are several biopolymers with interesting properties that could compete with conventional

plastics, like poly (butylene adipate-co-terephthalate) (PBAT) with a production capacity of around 300.000 tons in 2019.[1] This is a biodegradable aliphatic-aromatic polyester with mechanical properties similar to low-density polyethylene (LDPE), but it presents low water vapor barrier properties.[2] On the other hand, polyhydroxyalkanoates (PHAs) with a production capacity of around 25.000 tons in 2019,[1] considered as a potential replacement for polypropylene (PP) due to their similar thermal and mechanical properties (T_m 176°C, tensile strength around 42 MPa), but the processing temperature range of PHAs is limited and its elongation at break is more than 98% lower than PP.[3] In addition, poly(butylene succinate) (PBS) with a production capacity of around 90.000 tons in 2019,[1] is an interesting aliphatic polyester that it could be used in the food packaging field [4] due to its good processing capacity, thermal and chemical resistance, biodegradability and good mechanical properties, comparable to those of polyethylene (PE) and polypropylene (PP),[5] but it presents low elongation at break. For this reason, several studies have been focused to enhance the limited properties of those biopolymers, i.e. using nanoparticles to improve their thermal and mechanical properties such as cellulose nanoparticles and halloysite nanotubes [6,7] or by blending with other biopolymers such as polycaprolactone (PCL) and PLA.[8,9]

This last one, Poly (lactic acid) (PLA), is also a promising biodegradable thermoplastic biopolymer with a production capacity of around 300.000 tons in 2019.[1] PLA is mainly used in medical applications, food packaging industry and 3D printing.[10–13] However, it presents a high rigidity and fragility compared with other biopolymers. Therefore, the search for conferring ductility to PLA continues to be an interest research topic. Moreover, high temperature resistance, hydrophobicity and melt flow rate, are limited properties that have led to the research and development of new sustainable polymer formulations based on PLA and other materials.[14–16] In this context, in order to enhance those properties and open the possibility to find new and innovate applications, some methods based on the surface modifications has been employed.[17–19] Chemical treatment and different materials and additives such as, vegetable oils and fatty acids, have been used with the purpose of providing ductility and enhance PLA processability.[20,21] Binary and ternary formulations have been the most common. For example, Ferri et al., employed maleinized linseed oil (MLO) as plasticizer, which caused an increase in the mobility of the polymer chains of PLA. Therefore, a reduction of the T_g and the peak of cold crystallization was found, which had a direct impact on the increment of the crystallinity and consequently improved the ductile properties of the obtained materials.[22] In addition, Bhasney et al., studied the plasticizing effect of coconut oil on PLA, and found remarkable results on the increment of elongation at break by the increasing amount of coconut oil added.[23]

Moreover, Moustafa et al., revealed the excellent possibility of incorporation of natural antibacterial rosin in a blend of PLA/PBAT for food packaging and bio-membrane applications.[24] In this sense, the use of materials and additives from natural origin draws attention of the bioplastic industry, due to the possibility of obtaining modified properties without compromising the eco-friendly characteristics of the material.

Natural resin from pine trees (gum rosin-GR) and derivatives are part of the renewable resources use as modifier agents in the development of biobased polymers for industrial applications.[25,26] GR is a natural resin extracted by exudation of the pine trees.[27] It consists in a complex mixture of terpenes, neutral components and resin acids, mostly abietic acid (15-20%).[28,29] GR and its derivatives are used in paper and printing ink industry, although they are also used in different applications, such as coating and as an adhesive. [30,31] The GR derivatives are obtained by chemical modifications, such as esterification, dimerization, isomerization or hydrogenation, with the mean propose of provide thermal stabilization at different scale and color changes.[30,32] In a previous work, GR and two derivatives were used in the processability and mechanical performance improvement of a Mater-Bi biopolymer obtaining interesting results for industrial application.[33] Kaavessina et al., used GR as a plasticizer of PLA in a content of 5, 10 and 20 %, they only analyzed the rheological properties that determined the plasticizing effect by reducing the complex viscosity and improving the biodegradability of the mixtures.[34]

In this context, the aim of this work was to evaluate the changes occurred in melt flow index, wettability, thermal and mechanical properties of poly (lactic acid) after its melt–compounding with GR and GR derivative (pentaerythritol ester of gum rosin) in different contents, using different techniques like tensile, flexural and dynamic mechanical analysis, among other techniques, considering the difference between both resins.

2 Experimental

2.1 Materials

Poly (lactic acid) (PLA) Ingeo Biopolymer ™, commercial grade 6201D obtained from NatureWorks LLC (Minnetonka, USA) was used as the thermoplastic matrix. This grade contains 2% D-lactic acid. It is characterized by having a density of 1.24 g cm^{-3} and a melt flow index (MFI) in the range of 15-30 g / 10 min (210 ° C, 2.16 kg). As additives, colophony and a derivative were used: gum rosin (GR) obtained from Sigma-Aldrich (Móstoles, Spain), its physical appearance is dark yellow in solid fragments shape at room temperature (level of purity of 99%), its molecular formula is $C_{20}H_{30}O_2$ and it has a molecular weight of 302 g/mol. Its softening point is between 40 - 50 °C and its melting temperature is between 66.5 - 93.4 °C at an approximate pressure of 1,103.0 hPa and it is characterized by having a relative density of 1.034 g cm^{-3} at 20 °C.[35] Pentaerythritol ester of gum rosin (PEGR), under the trade name Unik Tack P100, supplied by United Resins - Produção de Resinas S. A. (Figueira da Foz, Portugal). PEGR is a chemically modified resin. This modification consists in the conversion of the carboxyl groups, present in the gum rosin abietic acid, into an ester (esterification process) through the chemical reaction with pentaerythritol alcohol. This modification increases the molecular weight and the softening and melting temperature of the resin, having a direct impact in the compatibility of the resin and therefore increases its stickiness level and viscosity when is melted. Pentaerythritol ester of gum rosin has a molecular weight of 1469 g/mol, a relative density of 1.034 g cm^{-3}. Its softening point is between 50 – 60 °C and its melting temperature is between 96 -100 °C.

2.2 Preparation of the samples

Prior to materials processing, pellet of PLA and resins were premixed by manual agitation in plastic bags according to each PLA formulations with the varying contents of GR and PEGR prepared. Subsequently, the materials were dried for 12 hours at 40 °C in a dehumidifier oven model MDEO from Industrial Marsé (Barcelona, Spain). In order to obtain homogeneous mixtures, the different formulations were processed in a co-rotating twin-screw extruder, with a length-to-diameter ratio L/D 24, from Dupra, S.L. (Alicante, Spain). The temperature profile programmed from the feed hopper to the material outlet nozzle was 150, 160, 170 and 180 °C, with a screw speed of 20 rpm. The extruded materials, summarizes in **Table 1**, were milled and then injected-molded in standard test specimens in a Sprinter 11t injection machine from Erinca S.L (Barcelona, Spain), using a temperature profile of 175 °C (chamber) and 185 °C (injection nozzle), with a filling and cooling time set on 2 and 16 s, respectively. Two types of test specimens were obtained from the injected-molded process; standard specimens in dumbbell shape "1BA" used in tensile characterization according to ISO 527 [36] and standard rectangular specimens (80 x 10 x 4 mm^3) used in flexural characterization.

Table. 1. Composition of the formulated materials. GR and PEGR were added in phr of PLA content.

Polymeric matrix	Resin	Resin content (phr)		
		5	10	15
PLA	GR	PLA/GR_5	PLA/GR_10	PLA/GR_15
	PEGR	PLA/PEGR_5	PLA/PEGR _10	PLA/PEGR _15

2.3 Melt flow index measurements

The measurements of the melt flow index (MFI) were made in a Metrotec brand plastometer model Ars Faar, according to ISO 1133 [37] at 190 °C and a nominal load of 2.16 Kg. After the injection process, the specimens were milled and used in the MFI tests.

2.4 Wettability and Water absorption

The wettability was evaluated by measuring the water contact angle on the surface of the solid samples. The samples were rectangular injected-molded specimens sizing 80 x 10 x 4 mm^3. The tests were carried out at room condition (24 °C and relative humidity of 35%) with an Easy Drop Standard goniometer FM140 (Krüss GmbH, Hamburg, Germany). It is equipped with a monochrome camera and a control software for the measure evaluation (Drop Shape Analysis SW21; DSA1). Five drops of distilled water were randomly adding onto the solid samples surface with a micro syringe and measured, the average values of three measurements for each drop were used to calculate the contact angles.

Furthermore, the water absorption of neat PLA and PLA formulations with varying contents of GR and PEGR was determined in accordance with ISO 62 guideline,[38] using the same type of specimens prepared for the wettability tests. To obtain average values of water absorption, three different samples for each formulation were tested. Before performing the test, samples were storage for 48 hours at 50 °C in a dehumidifier oven model MDEO from Industrial Marsé (Barcelona, Spain), in order to dried them and obtain constant weight. Subsequently, samples were immersed in distillated water at room condition (24 °C and relative humidity of 35%) for a period of 4 weeks and the weight change was measured every two days during the first week, then the weight change was measured every week. The percentage mass change (*c*), due to the water absorption, was calculated by using the following Eq. 1.

$$c = \left(\frac{M_f - M_i}{M_i}\right) x\ 100 \qquad \textbf{(Eq. 1)}$$

Where M_f is the final weight after a certain immersion period and is M_i is the initial weight of the sample before immersion.

2.5 Color Measurements

These properties were evaluated by using a Colorflex-DIFF2 45°/0°spectrophotometer from Hunter Associates Laboratory, Inc. (Reston, Virginia, USA). The samples used for the measurement were rectangular specimens sizing 80 x 10 x 4 mm^3 obtained by injected-molded process. The instrument was calibrated with a white standard tile and the average value of three measurement at random positions over the samples surface was calculated. The color coordinates, L* (lightness), a* (red - green) and b*(yellow - blue) were used to determine the total color differences (ΔE) induced by the presence of GR and PEGR in the injected samples when compared to the control PLA by following Eq. 2:

$$\Delta E = \sqrt{(\Delta L^*)^2 + (\Delta a^*)^2 + (\Delta b^*)^2} \qquad \textbf{(Eq. 2)}$$

Yellowness index (YI) was used to evaluate the color change from clear to yellow. It was calculated to determine the change of the material yellowness due to the incorporation of GR and PEGR with respect of neat PLA.

2.6 Thermal Characterization

The materials thermal characterization was carried out in a differential scanning calorimeter (DSC) Mettler-Toledo 821 (Schwerzenbach, Switzerland). To examine the main thermal transitions of neat PLA and PLA formulations, a thermal analysis was programmed in three cycles: (1) initial heating from 25 to 180 °C, (2) cooling from 180 to -50 °C and (3) second heating from -50 to 350 °C. To evaluate GR and PEGR additives, the thermal analysis was programmed with an initial heating from 30 to 90 °C, a cooling from 90 to 30 °C and a second heating from 30 to 130 °C. Both thermal analyses were

done at a heating-cooling rate of 10 °C min^{-1}, in a nitrogen atmosphere (30 mL min^{-1}) using an average sample weight ranged from 6 to 8 mg placed in standard aluminum crucibles with a volume capacity of 40 µL. The degree of crystallinity (X_c) of the PLA and PLA formulations was calculated with equation (3).

$$X_C = \left[\frac{\Delta H_m - \Delta H_{cc}}{\Delta H_m^0 \cdot (1-w)}\right] \quad \textbf{(Eq. 3)}$$

Where ΔH_m is the melting enthalpy (Jg^{-1}), ΔH_{cc} is the cold crystallization enthalpy (Jg^{-1}), ΔH_m^0 represent the theoretical melting enthalpy of a full crystalline PLA *i. e.* 93.0 (Jg^{-1}) [39] and $(1 - w)$ corresponds to the weight fraction of PLA in the samples.

The samples thermal stability was evaluated by thermogravimetric analysis (TGA), conducted in a Linseis TGA PT1000 (Selb, Germany). The dynamic analysis of the decomposition profile of neat PLA and PLA formulations was done with a heating rate of 10 °C min^{-1}, from 40 to 600 °C, in a nitrogen atmosphere (30 mL min^{-1}) using an average sample weight ranged from 18 to 20 mg placed in standard alumina crucibles (70 µL). The onset degradation temperatures ($T_{5\%}$) were determined at 5% of mass loss, while temperatures of the maximum decomposition rate (T_{max}) were calculated from the first derivative of the TGA curves (DTG).

2.7 Mechanical Characterization

The tensile and flexural properties were determined under the ISO 527 and ISO 178 standards,[36 40] respectively, using an Ibertest electromechanical universal testing machine ELIB 30 (Madrid, Spain). The standard specimens used for tensile and flexural characterization were prepared as described in section 2.2. The tensile tests were performed with at 10 mm min^{-1} with a load cell of 5 kN, at room temperature. For the flexural tests, the rate was 5 mm min^{-1}, load cell of 5 kN and a separation of 64 mm between the support points. The impact resistance was determined on specimens without notches (injected-molded specimens sizing 80 x 10 x 4 mm^3), using a 6 J Charpy pendulum in an impact test machine from Metrotec, S. A, (San Sebastián, Spain), under ISO 179 standards.[41] Shore D hardness of the materials was carried out making three measurements for each sample and averaging the results, according to ISO 868,[42] using a durometer 676-D from Instruments J. Bot SA (Barcelona, Spain), at room conditions (24 °C and relative humidity of 35%).

2.8 Thermo-mechanical characterization

The dynamic mechanical analysis (DMTA) in torsion mode was performed on an AR G2 oscillating rheometer from TA Instruments (New Castle, USA), with an adaptation of specific clamps for fastening the tested specimens with approximate dimensions of 40 × 10 × 4 mm^3. The test temperature was programmed from 30 to 150 °C, at a heating rate of 2 °C min^{-1}, a frequency of 1 Hz and a maximum deformation (γ) of 0.1%.

In addition, Vicat softening temperatures (VST) and Heat deflection temperature (HDT) were measured in a Vicat/HDT Deflex 687-A2, Metrotec S. A (Sebastian, Spain), in a heating bath with silicone oil. The VST values were obtained using the B50 method of ISO 306.[43] The HDT measurements were obtained according to method A of ISO 75.[44] Both tests, VST and HDT were performed with rectangular injected-molded specimens sizing 80 x 10 x 4 mm^3.

2.9 Morphological Study

The morphology of the materials was observed through the microstructure of the fractured specimen surfaces of the impact tests, using a scanning electron microscope (SEM) to evaluate the dispersion of the resins in the polymeric matrix of PLA. A Phenom microscope from FEI Company (Eindhoven, The Netherlands) with an acceleration voltage of 5 kV was employed. Before the test, all samples were coated with a gold palladium alloy to make their surface conductive, on a Sputter Coater Emitech SC7620, Quorum Technologies (East Sussex, UK).

3 Results and discussion

3.1 Melt flow index measurement

The results shown in **Fig.**1 reveal the decrease occurred in the melt viscosity of the formulations, resulting in an increasing tendency of PLA melt flow index (MFI) as GR and PEGR content increase into the polymeric matrix. As it can be observed, addition of GR produces an MFI increment in higher proportion than that obtained for PLA with PEGR. For 5 phr content of GR, the MFI experiences an increment of 790% (115.3 g /10 min), while the addition of PEGR, in the same content, increases the MFI in 193% (37.6 g /10 min), compared to neat PLA value (13 g /10 min). Such increment in MFI values could be related to a lubricating effect produced by the resins into the PLA, facilitating the polymer chains mobility.[45,46] Moreover, the remarkable increase of MFI values in PLA formulations with GR, is associated with the low stability of the GR due to its unsaturation (lack of hydrogen bonds). This unsaturation makes GR susceptible to temperature, presenting low softening point (in the rage of 40 – 50 °C) and also a low molecular weight (in the rage of 296 – 302 g/mol),[47] compared to the PEGR. All these factors produce low viscosity of the melted mass and, therefore, they influence the MFI values. On the other hand, PEGR has higher softening point (in the rage of 50 – 60 °C) and higher molecular weight (in the rage of 1469 – 1480 g/mol), due to the chemical modification, which produce a higher viscosity of the melted mass.[48–50]

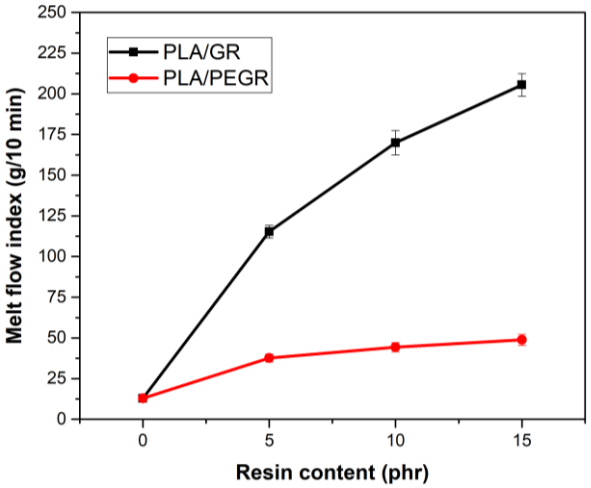

Fig. 1. MFI trends of PLA, PLA/GR and PLA/PEGR blends

3.2 Wettability and Water absorption analysis

By water contact angle measurement, it was studied whether the addition of GR and PEGR could have a positive effect on PLA wettability properties. As it can be seen in **Fig. 2**. Neat PLA presents a contact angle of 77.2 °. And the addition of GR led to decrease water contact angle of PLA, showing a decreasing tendency in the values with increasing amount of GR, reaching values of 72.4 ° for PLA with 15 phr GR content. However, the addition of PEGR led to obtain a stronger hydrophobic surface in the resulting material, evidenced by increased the contact angle value up to 88.6 ° in the mixture with 15 phr PEGR content, as shown in **Fig. 2**. The hydrophobic effect produced by PEGR in PLA, could occurs due to the ester formation from the carboxyl groups presents in rosin acid with pentaerythritol alcohol by means of esterification process. According to Siddiki et al., esters present limitations in the formation of hydrogen bonds, and therefore they are more hydrophobic than the corresponding carboxylic acids and alcohols.[51]

In addition, the water absorption evolution of neat PLA and PLA formulations with the varying content of GR and PEGR, is shown in **Fig. 3**. As it can be seen, the incorporation of GR to PLA significantly increases water absorption capacity thereof. This behavior is attributed to the hydrogen bonds formation between water molecules and carboxylic acids in GR. It is well known that; carboxylic acids are polar, and they do not dimerize in water, but due to the hydroxyl in the carboxyl group, they are able to form hydrogen bonds with water molecules.[52,53] Moreover, due to the low compatibility of GR and the polymeric matrix, their interaction could generates defects in the samples and, therefore, a greater amount of water is absorbed. The higher is GR content into PLA, the more hydrophilic it becomes (as it observes in the water contact angle measurements). On the other hand, the incorporation of PEGR increased the water absorption capacity of PLA, associated with the defect generated by PEGR saturations. However, those values are lower than observed for PLA/GR formulations due to the hydrophobic characteristics of PLA/PEGR formulations.

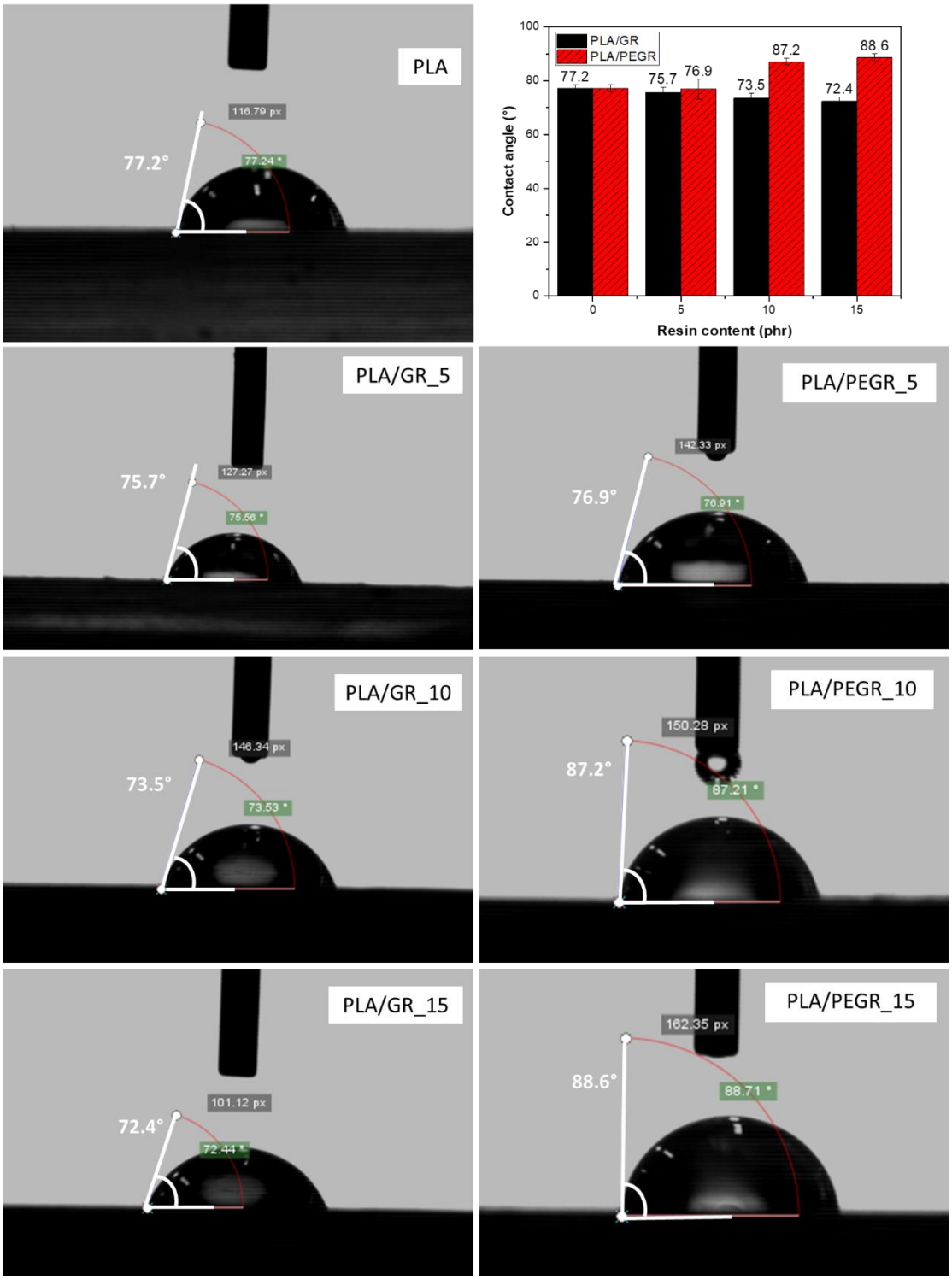

Fig. 2. Contact angle values for PLA, PLA/GR and PLA/PEGR blends.

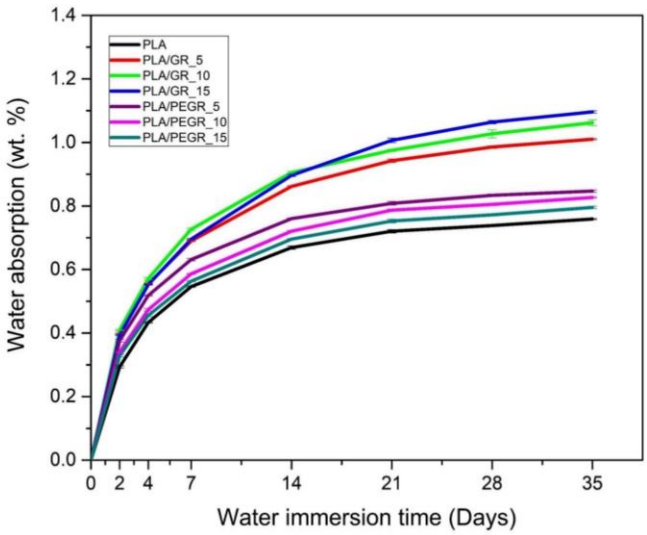

Fig. 3. Water absorption evaluation of neat PLA and PLA formulations with the varying content of GR and PEGR.

3.3 Color measurements

The color values obtained for the studied materials based on the CIELab* system, as well as the total color differences (ΔE) and yellowness index (YI) are shown in **Table 2**. The results obtained by colorimetry confirm that the addition of GR and PEGR to PLA increase the brightness in all samples, especially in the blends with PEGR, since L* values tend to increase from 38.3 (neat PLA) up to 85.1 (PLA/PEGR_15). Moreover, it should be noted that the high values of 85.1 in L* coordinate for PLA/PEGR_10 and PLA/PEGR_15, together with the low values of b*, 9.4 and 9.7, respectability, could be due to the milky color exhibit by the samples, (**Fig. 4**). The negative values of a* coordinate, clearly means that there is not presence of red color on the samples. However, the increase trend in b* values with the addition of GR, confirm the yellowish tonality in the samples. This tonality is more intense with the greater amount of GR added to PLA, reaching values of 29.8 for PLA/GR_15 compared with neat PLA. Regarding the total color difference ΔE, all samples showed a significant change by the addition of GR and PEGR, with tendency to increase as the amount of GR and PEGR increases. Samples with GR show values in the range of 9 to 37, while the samples with PEGR show values in the range of 30 to 47.5. The results of the yellowness index (YI), shows that the high values (from 27 to 60) are found in the materials that contains GR as additive. This effect is due to the yellow tone of the additive, also confirmed with the b* coordinate values. The low YI values, in the range of 10 -17.4 for the PEGR blends, suggest that this resin have lower influence in the yellow tone of the samples than GR resin. Due to the color induced by the studied additives, shown in **Fig. 4**, GR and PEGR could be considered as natural pigments for industrial final products. In some cases, the colored materials are needed for specific applications (when the product must be protected from light). Therefore, the use of GR and PEGR can be considered a viable option to modify the color of some plastic materials due to its natural origin and innocuous characteristics.

Table. 2. Color measurement for the studied samples

Samples	L*	a*	b*	ΔE	YI
PLA	38.2 ± 0.3	-0.2 ± 0.1	2.4 ± 0.4	0	8.9 ± 1.6
PLA/GR_5	42.3 ± 0.5	-3.3 ± 0.1	9.9 ± 0.5	9.1 ± 0.5	27.1 ± 1.8
PLA/GR_10	43.1 ± 0.5	-3.5 ± 0.2	17.6 ± 0.4	16.1 ± 0.7	48.3 ±1.2
PLA/GR_15	63.1 ± 0.3	-3.6 ± 0.4	29.8 ± 0.4	37.1 ± 0.6	60.0 ±1.8
PLA/PEGR_5	68.4 ± 0.6	-4.2 ± 0.1	6.3 ± 0.4	30.7 ± 0.7	10.7 ± 0.8
PLA/PEGR_10	85.1 ± 0.7	-2.7 ± 0.1	9.4 ± 0.2	47.4 ± 0.7	16.6 ± 0.5
PLA/PEGR_15	85.1 ± 0.7	-2.4 ± 0.1	9.7 ± 0.9	47.5 ± 1.0	17.4 ± 0.7

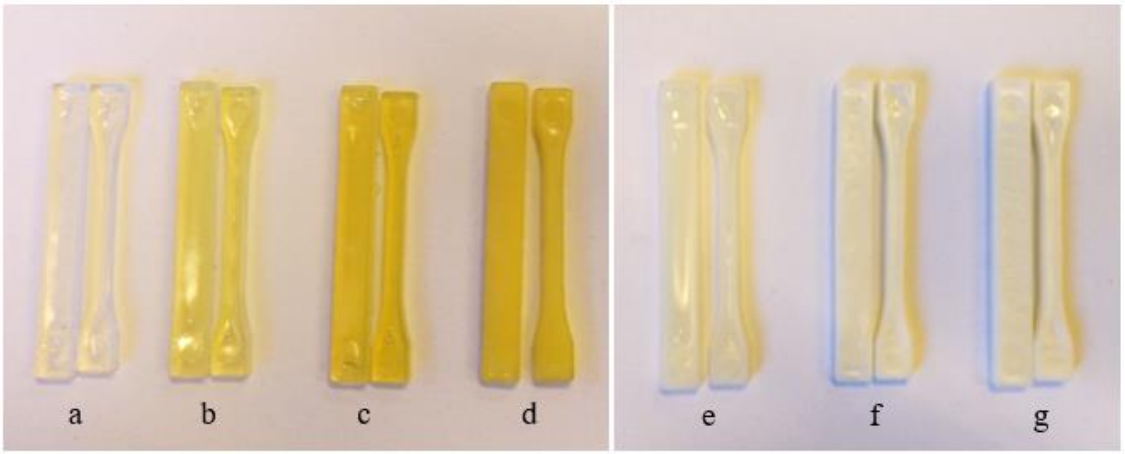

Fig. 4. Surface appearance of the test samples obtained by injection molding made of **a)** neat PLA; **b)** PLA/GR_5; **c)** PLA/GR_10; **d)** PLA/GR_15; **e)** PLA/PEGR_5; **f)** PLA/PEGR_10 and **g)** PLA/PEGR_15.

3.4 Thermal properties

Fig. 5(a) Show the DSC second heating curves from neat PLA and PLA formulations with the varying content of GR and PEGR. A summary of the main thermal parameters obtained in the second heating run is shown in **Table 3.** Regarding the changes occurred in the glass transition temperature (T_g), it can be observed how the incorporation of GR and PEGR into PLA results in slightly decrease of neat PLA T_g (63.5 °C), showing a tendency to decrease with increasing GR content, down to 55.9 °C for PLA with 15 phr GR, almost 8 °C less than neat PLA. Meanwhile, PEGR decreased T_g in about 3 °C for PLA with 10 phr PEGR (60.1 °C). This slightly decrease in T_g is attributed to a lubricating effect produce by the GR and PEGR in the PLA matrix, that induce a higher mobility to its polymeric chains at lower temperature. Literature refers that a decrease in T_g is directly related to greater mobility of polymer chains.[22,23] In addition, the cold crystallization temperature (T_{cc}) presents similar decreasing tendency to that observed for T_g. The exothermic peak located at 105.8 °C corresponding to neat PLA cold crystallization, is slightly shifted to lower temperatures in all formulations, reaching values of 98 °C for PLA with 15 phr PEGR. This is associated with the lubrication effect produced by PEGR. As shown in **Table 3**, neat PLA exhibits a crystallinity (X_c) of 9.6 %, which decrease down to 7.3 % and 6.3 % for PLA with 15 phr GR and PEGR, respectively.

DSC thermograms of gum rosin (GR) and pentaerythritol ester of gum rosin (PEGR) are shown in **Fig. 5**(b). As it can be observed, GR presents a baseline step located at lower temperature to that shown for PEGR. Both baseline steps, with no other exothermal or isothermal transition over the second heating cycle, are associated with the glass transition temperature ($T_{g)}$ of the components. For GR the baseline step occurs between 40.5 °C and 45 °C, meanwhile, PEGR shows the baseline step between 50.6 °C and 61°C, about 15 °C difference between the inflection point temperature of GR (42.4 °c) and the inflection point temperature of PEGR (56.7 °C). As it was mentioned before, PEGR is rosin ester of gum rosin with higher thermal stability, therefore, a higher T_g value was expected respect to GR. It is worthy to mention that, gum rosin is a natural complex mixture obtained from the oleoresin of pine trees and its thermal properties could variate depending on the method and process of extraction. In a prior study, Cabaret et al., has reported rosin softening point temperature around 43.8 °C.[54]

Table. 3. Thermal properties of the studied formulations

Samples	**DSC**						**TGA**	
	T_g (°C)	**T_{cc} (°C)**	**ΔH_{cc} (Jg^{-1})**	**T_m (°C)**	**ΔH_m (Jg^{-1})**	**X_c (%)**	**$T_{5\,\%}$ (°C)**	**T_{max} (°C)**
PLA	63.5	105.8	17.9	172.5	26.8	9.6	332.3	374.3
PLA/GR_5	61.1	103.6	21.3	170.1	28.7	8.4	319.3	372.6
PLA/GR_10	60.1	102.3	24.6	168.2	31.3	7.9	300.6	371.3
PLA/GR_15	59.5	102.5	26.4	168.0	32.2	7.3	298.4	370.8
PLA/PEGR_5	61.0	103.5	24.7	172.2	31.0	7.0	335.0	371.8
PLA/PEGR_10	60.4	99.8	28.9	170.2	34.6	6.7	337.9	373.5
PLA/PEGR_15	62.6	98.0	19.2	170.1	24.3	6.3	340.0	373.8

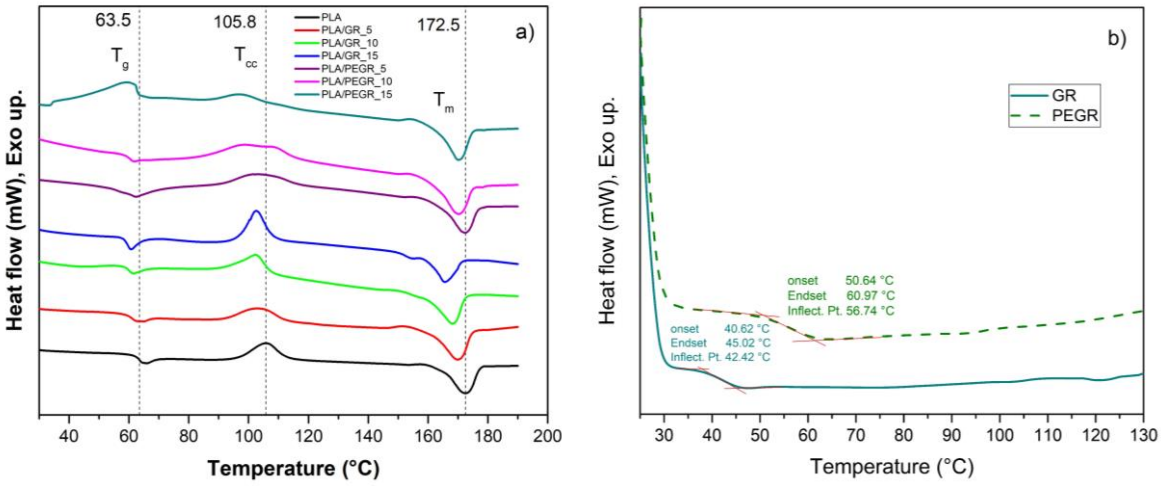

Fig. 5. a) DSC curves of the second heat from neat PLA and PLA/formulations; **b)** DSC curves of GR and PEGR.

Regarding the thermal stability assessment, **Fig.** 6 shows the thermo-gravimetric (TGA) and derivative thermo-gravimetric (DTG) curves of neat PLA and PLA formulations with the varying content of GR and PEGR. Meanwhile, **Table** 3 shows the onset degradation temperature values ($T_{5\%}$) determined at 5% of mass loss and the temperature values of the maximum decomposition rate (T_{max}), calculated from the first derivative of the TGA curves.

As it can be observed in **Fig. 6**(a), neat PLA degrades in a single step process with onset degradation temperature ($T_{5\%}$) of 332.3 °C, as it was formerly reported by Ferri et al.[55] The addition of GR led to a noticeable reduction of the onset temperature degradation between 13 °C (PLA with 5 phr GR) and 34 °C (PLA with 15 phr GR). On the other hand, PEGR addition led to slightly increase this onset temperature degradation up to 5.6 and 7.7 °C for PLA with 10 and 15 phr PEGR, respectively. Those results suggest that PEGR enhance the thermal stability as it delayed the degradation/decomposition process to higher temperature. Moreover, this behavior is associated with the intrinsic thermal characteristic of PEGR, which present higher thermal stability than GR due to its modification (esterification). Similar behavior has been observed by Aldas et al., when adding GR and derivatives to a bioplastic composite based on starch and aliphatic/aromatic polyesters.[33] Nevertheless, even though GR and PEGR influenced the onset degradation temperature, they did not produce significant effect in the temperature values of the maximum decomposition rate, represented by the peaks between 370.8 and 374.3 °C on the derivative thermo-gravimetric (DTG) curves (Fig. 6 b). This last behavior is attributed to the characteristic of the polymer matrix (PLA), which is not highly affected by the amount of GR and PEGR added and keeps its maximum decomposition temperature values in a relatively narrow range. However, other additives such as chain extenders, can cause large changes in the maximum decomposition temperature of PLA.[56]

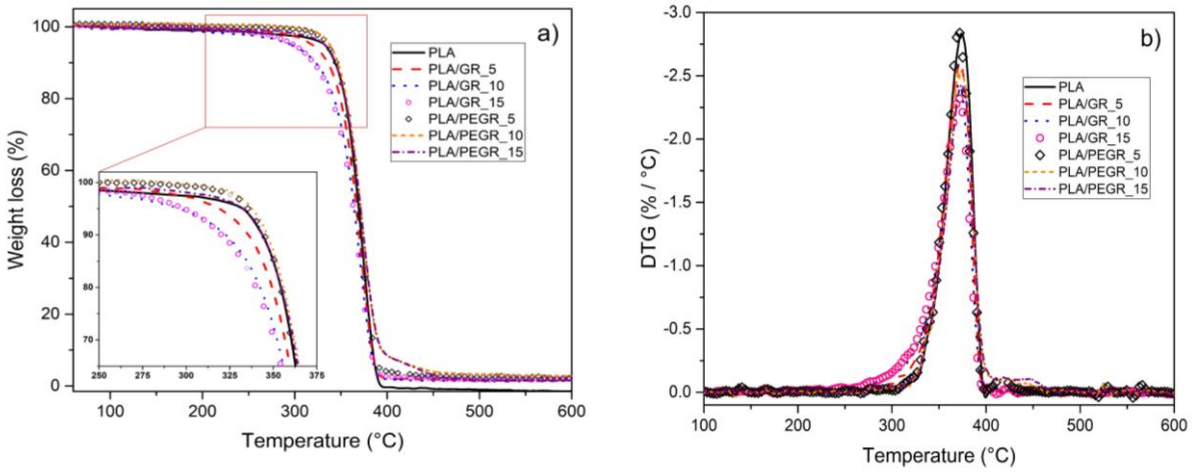

Fig. 6. a) TGA and **b**) DTG of neat PLA and PLA formulations with varying contents of GR and PEGR.

3.5 Mechanical properties

The tensile properties evaluation of neat PLA and PLA formulations with the varying contents of GR and PEGR, is shown in **Fig. 7**. As it can be seen, tensile strength behavior of PLA/GR and PLA/PEGR blends are similar in both cases, GR and PEGR incorporation lead to decrease the tensile strength values respect to that shown for neat PLA (64 MPa). It is noticeable that, addition of GR into PLA produces a greater decline in the tensile strength values compared to PEGR (**Fig. 7a)**. For equal contents of GR and PEGR (5 phr) tensile strength values decrease down to 59.5 and 62.3 MPa, respectively, with about 3 MPa difference between them. However, as contents of GR and PEGR increase, the difference between their tensile strength values are more noticeable, dropping to 21.2 MPa (percentage decrease of 66.8 %) and 54 MPa (percentage decrease of 15.6%) for PLA with 15 phr GR and PEGR, respectively, with respect to the strength of neat PLA. This drop in tensile strength is associated with a beginning of a phase separation in the blends containing GR and PEGR above 5 phr due to a saturation effect, which weakens the polymer by generating stress concentration.[22] [33] Kaavessina et al., have formerly reported the plasticizing effect of gum rosin into PLA matrix when added in lower contents.[34] Therefore, above 5 phr contents the saturation effect is possible. We could probably talk about a plasticizing effect in the exclusive case of PLA with 5 phr PEGR, where remarkable decrease in the tensile modulus down to 1495 MPa (percentage decrease of 27 %) (**Fig. 7b**) as well as a slightly increase in the elongation at break up to 7.9 % (**Fig. 6c**) is observed, both compared with the tensile strength and elongation at break values obtained for neat PLA (2060 MPa) and (5.9 %), respectively. Ferri et al., have reported a plasticization effect of a biobased epoxidized fatty acid ester into PLA by describing the phenomenon in the same way, an increment in the elongation at break and a reduction in the tensile modulus and tensile strength of PLA formulations.[57] It is worth to notice, how the elongation at break for PLA with 10 and 15 phr GR contents decrease considerably to 3.1 and 1.7 %, respectively. This behavior could be explained for the fact that 5 phr content is the maximum amount of GR assimilated by the polymer matrix before starting the saturation. Moreover, Pavon et al., have evaluated the effect of gum rosin over polycaprolactone (PCL) matrix, obtaining good plasticizing effect and enhanced thermal stability of PCL due to the GR incorporation.

A broader analysis of the stress-strain curves (Fig. 8), shows the deformation characteristics of neat PLA and PLA formulations. As it can be observed, addition of GR (in the rage of 5 – 15 phr contents) reduces the PLA strength capacity, evidence by the reduction of the tensile strength, which in turn accompanied by the decrease in the elongation at break, decreases the elastic zone of the material.[58] Nevertheless, even though PLA with 5 phr GR content was affected by the reduction of strength and elongation at break, it slightly increased its stiffness, in accordance with the slightly increment of the tensile modulus. This behavior could explain the loss of impact resistant.

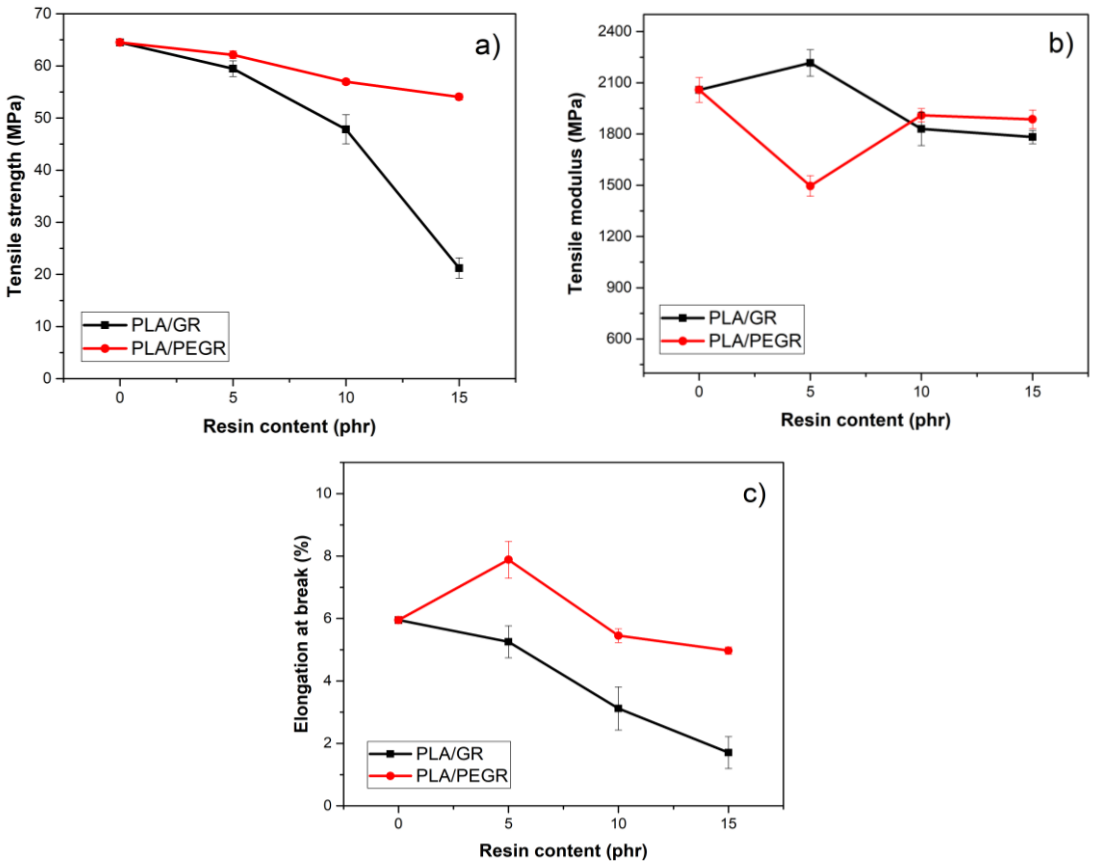

Fig. 7. Evaluation of mechanical tensile properties of PLA with 5, 10 and 15 phr of GR and PEGR resins: **a**) Tensile strength; **b**) Tensile modulus; **c**) Elongation at break.

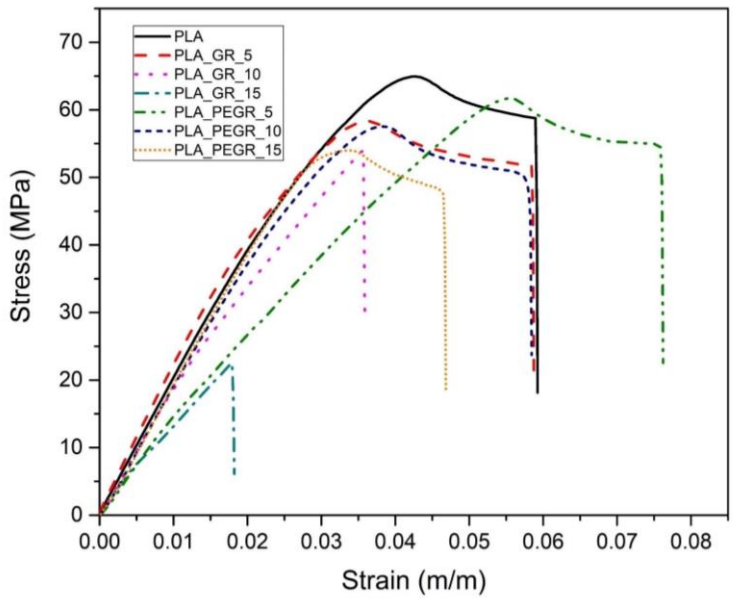

Fig. 8. Stress–Strain curve of neat PLA and PLA formulations with the varying content of GR and PEGR.

Fig. 9 shows the flexural properties evaluation of neat PLA and PLA formulations with the varying contents of GR and PEGR. Neat PLA is characterized by having a flexural strength of 117.3 MPa and a flexural modulus of 3299 MPa. A decreasing tendency in the flexural strength values was observed by the incorporation of GR and PEGR into PLA polymeric matrix. As it is shown in **Fig. 9a**, PLA formulations present almost a linear decrement in the flexural strength with increasing amount of PEGR, from 112 MPa (percentage decrease of 4.5 %) to103.3 MPa (percentage decrease of 11.9 %), this is for PLA with 5 and 15 phr PEGR, respectively, both respect to neat PLA. Meanwhile, the addition of GR led to reduce flexural strength in higher proportion than PEGR. For PLA with 5 and 15 phr GR the decrease occurs down to 12.4 and 67 %, (102.7 and 38.7 MPa, respectively). Regarding flexural modulus, **Fig. 9b**, it can be observed how over 5 phr contents of GR and PEGR the flexural modulus behavior is completely different, GR led to increase up to 3646 MPa and PEGR led to slightly decrease down to 3175.5 MPa (formulations with 15 phr GR and PEGR). This flexural strength reduction is directly related to the addition of GR and PEGR. As their contents increase, the greater is the weakness in the material due to saturation. According to G. Odian, the rigidity of a polymer is associated with the modulus and the polymer resistance level to be deformed.[59] J. A Sauer holds that crystalline regions give stiffness and resistance to polymers; [60] consequently, it is confirmed that addition of GR and PEGR leads to reduce the stiffness and therefore the flexural strength of PLA, especially above 5 phr contents. As it was also observed in tensile properties behavior.

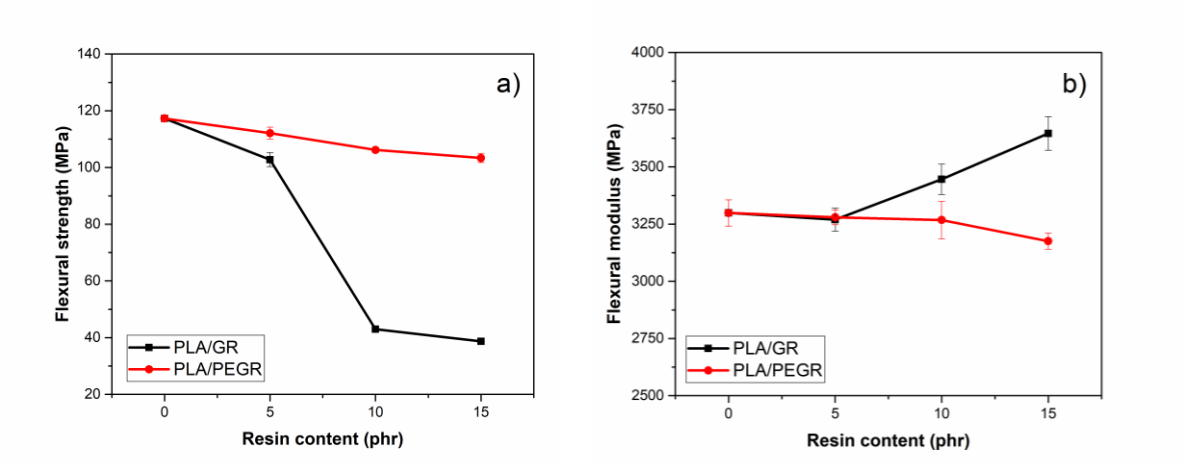

Fig. 9. Evaluation of mechanical flexural properties of PLA with 5, 10 and 15 phr of GR and PEGR resins: **a)** Flexural strength; **b)** Flexural modulus.

From the Charpy's impact resistance of the formulations studied, shown in **Table 4**, it is possible to confirm that neat PLA is characterized by having an impact energy absorption value of 37.6 kJ m^{-2}. However, physical blends of PLA with GR and PEGR led to a noticeable decrease in the energy absorption in all formulations, except for PLA with 5 phr PEGR that showed an impact resistance of 38.5 kJ m^{-2} (percentage increase of 2.4 %), similar value to that obtained for neat PLA. The impact resistance decrement, in the rage of 21 - 6.36 kJ m^{-2} for PLA with increasing contents of GR, as well as the reduction in

the range of 23-17.4 for PLA with PEGR over 5 phr contents, could indicate poor miscibility between components due to the saturation of the resin, which leads to clear phase separation as shown in the morphological study results. Moreover, according to the tensile properties results we said that adding GR to PLA leads to reduce its tensile strength and elongation at break, therefore, a remarkable decrease in the impact resistance of PLA/GR blends was expected, because of the alleged fragility. On the other hand, despite the decrease in the impact resistance values of PLA with 10 and 15 phr PEGR contents, the slight increment with 5 phr PEGR content, can be linked to PEGR incorporation into PLA polymeric matrix, which provides greater cohesion between molecules and absorbs more energy before breaking, in good accordance with the slight increase of elongation at break in the tensile properties evaluation. A similar behavior of the gum rosin and derivatives was reported by Aldás et al., who used gum rosin (GR) and derivatives to modify a commercial thermoplastic starch (TPS), describing a good chemical interaction of TPS and modified resin, as well as a high cohesion between the molecules of both materials by the modified resin effect.[33]

Table 4 also shows the hardness, Vicat softening temperature (VST) and Heat deflection temperature (HDT) values of PLA/GR and PLA/PEGR formulations compared with neat PLA. No significant changes were observed for Shore D hardness, where all samples including neat PLA, presented values close to 84. In relation to VST, neat PLA showed a value nearly to 58 °C, which decreased sequentially by the increasing amount of GR down to 53.8 °C for PLA with 15 phr GR. This behavior confirms the effect of GR on PLA, which induces greater mobility of the polymer chains due to GR susceptibility to temperature as a result of its low softening point (in the rage of 74 – 76 °C) and low molecular weight (in the rage of 296 – 302 g/mol). Whereas, PLA/PEGR samples presented VST values around 57 °C. Due to the susceptibility of GR to temperature, the HDT values for PLA formulations with GR were also influenced, almost 2°C lower in PLA formulation with the maximum GR content was obtained.

Table. 4. Variation of Charpy's impact resistance, Shore D hardness, VST and HDT of PLA with varying content of GR and PEGR resins.

Samples	Charpy's impact resistance (kJ m^{-2})	Shore D hardness	Vicat softening temperature, VST (°C)	Heat deflection temperature, HDT (°C)
PLA	37.6 ± 0.1	83 ± 0.6	57.9	58.6
PLA/GR_5	21.8 ± 1.6	83 ± 1.0	55.0	57.0
PLA/GR_10	13.9 ± 0.6	84 ± 0.6	54.5	56.4
PLA/GR_15	6.3 ± 1.0	84 ± 0.6	53.8	56.0
PLA/PEGR_5	38.5 ± 0.6	84 ± 1.0	57.6	57.5
PLA/PEGR_10	23.3 ± 0.9	83 ± 1.2	56.9	58.0
PLA/PEGR_15	17.4 ± 0.4	83 ± 1.0	57.7	57.7

3.6 Thermomechanical properties

Fig. 10 shows the variation of the storage modulus (G') and the damping factor (tan δ) of neat PLA and PLA formulations with the varying contents of GR and PEGR as a function of temperature. Since the type of PLA used for this study is semi-crystalline, the beginning of the curves of G' presents high values (around 2 GPa). In the glass transition interval, the modulus is significantly reduced to values around 55 MPa, and after 90 °C the storage modulus experiences an increase due to the cold crystallization process. PLA with different content of GR presents a similar G' values to that of neat PLA at the beginning of the test, however, it begins to decrease before the neat PLA, which indicate that T_g transition is having place at lower temperature due to GR incorporation, as can be seen in **Fig. 10a**. Then, the storage modulus values increase again around 60 MPa, from 80°C due to the crystallization process, which starts at lower temperatures than PLA, as the GR content increases. The T_g was determined by the peak of tan δ, which is shown in **Fig. 10b**. As it can be confirmed, the T_g slightly decrease by the incorporation of GR in the PLA samples, decreasing from 65.7 °C to 63 °C in the PLA/GR_5 and T_g for PLA/GR_10 and PLA/GR_15 decline to 62 °C. The same behavior of T_g reduction was also observed in the DSC assessment, where the T_g value decreased as the GR content increased. For PLA/PEGR samples no significant changes were observed, since thermal transitions occur in identical way as neat PLA. Regarding the T_g for PEGR formulations, similar values were observed between 65.8 and 66.6 °C.

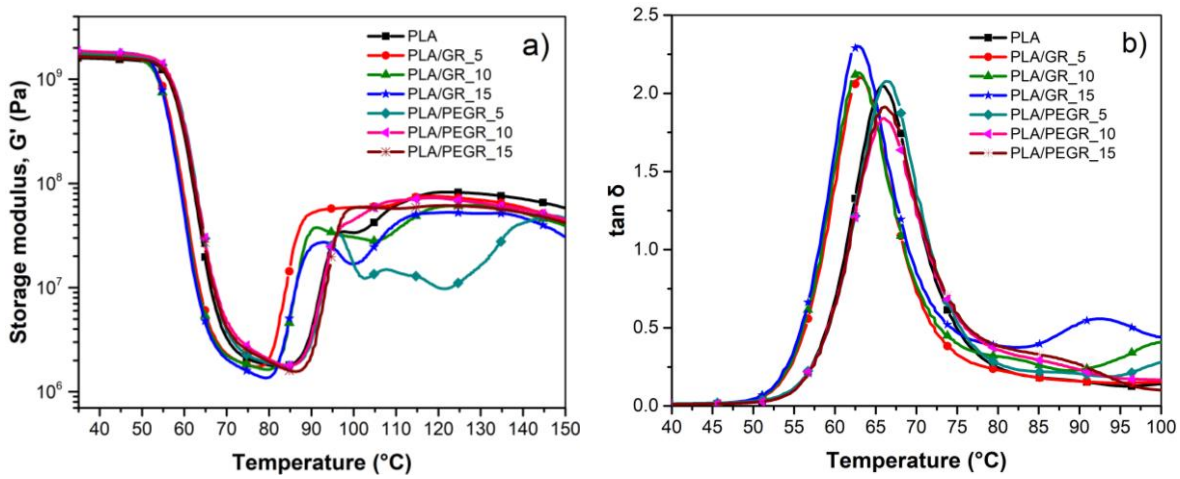

Fig. 10. Evaluation of DMTA results of PLA with different content of GR and PEGR resins: **a)** Storage modulus; **b)** Damping factor.

3.7 Morphology of the studied formulation í

Fig. 11 shows SEM images of the surface of the studied samples. As can be seen in **Fig. 11 a** and **b**, neat PLA presents a typical fracture with a partially smooth surface due to the low plastic deformation suffered, a fact that characterizes PLA as a relatively fragile polymer. The blend of PLA with 5 phr of GR (**Fig. 11c**), presents a surface with less

roughness than neat PLA. This confirms the increased fragility of the PLA as observed in the mechanical properties. In addition, it can be observed the presence of small granule formations corresponding to the GR resin added (dispersed phase in the polymer matrix of PLA). The number of granules increases with the increasing content of GR added. Unlike the morphology shown by the PLA/GR blends, the PLA/PEGR blends show a clear increment in the granule size of the dispersed phase, formed due to the saturation of the PEGR. The saturation increases as the amount of PEGR added increases, therefore, the resin added to the formulation acts as a stress concentrator, causing the decrease in the mechanical properties of the PLA, as it was observed in the mechanical characterization results in **Fig. 7**. Finally, in **Fig. 12**, it can be clearly observed how the craters and granules formed by the PEGR resin do not generate good cohesion in the polymer matrix, which confirms the saturation of the resin in the PLA.[26]

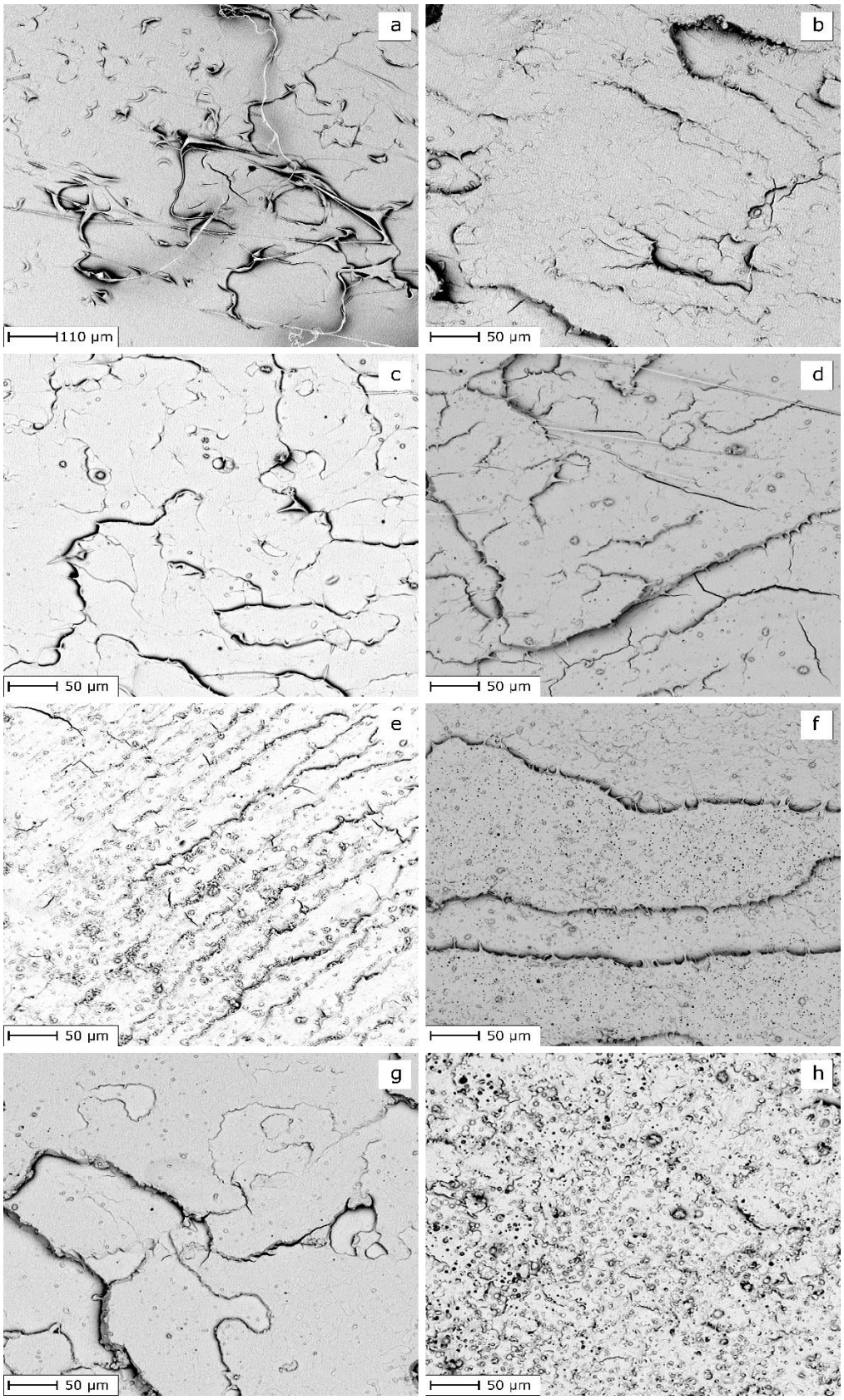

Fig. 11. SEM images of studied formulations: **a** and **b)** neat PLA at 1000x and 2000x; **c)** PLA/GR_5; **d)** PLA/PEGR_5; **e)** PLA/GR_10; **f)** PLA/PEGR_10; **g)** PLA/GR_15; **h)** PLA/PEGR_15, at 2000x of zoom.

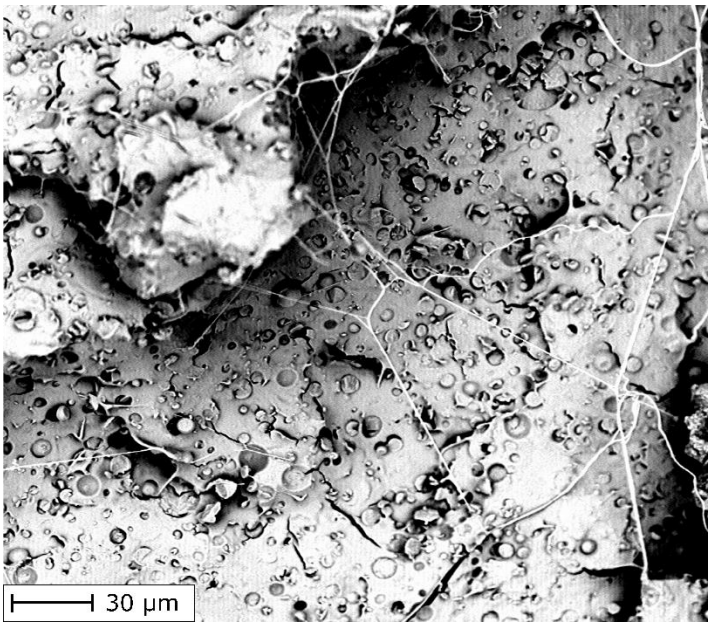

Fig. 12. SEM imagen of PLA/PEGR_15 at 3200x.

4 Conclusions

The present study has allowed to evaluate the effect of incorporating GR and PEGR into PLA polymeric matrix in contents of 5, 10 and 15 phr. Obtained results reveals a lubricating effect over PLA polymeric chains by the minimum content of GR and PEGR added (5 phr), obtaining greater processability of the formulations. Meanwhile a saturation effect is produced when GR and PEGR is added above 5 phr content. In addition, the incorporation of PEGR led to obtain a strong hydrophobic surface, evidenced by the increment of the water contact angle values in more than 10° with PEGR above 5 phr contents. TGA results show that PEGR addition delayed the PLA thermal degradation process to higher temperature, increasing the onset temperature ($T_{5\%}$) in more than 7 °C for PLA with 15 phr PEGR. Meanwhile, GR accelerated the thermal degradation by reducing the onset temperature ($T_{5\%}$) in more than 30°C (PLA with 15 phr GR). It was observed that GR increased the water absorption capacity of PLA (0.76 %) up to 1.1 % with the maximum PEGR content added.

Acknowledgements

This research was supported by the Ministry of Economy and Competitiveness-PROMADEPCOL Ref: (MAT2017-84909-C2-2-R). Authors also want to acknowledge the postdoc contract offered to José Miguel Ferri by the Generalitat Valenciana, which project title is "BIONANOCOMPOSITES BASADOS EN MEZCLAS DE PLA Y TPS CON MEMORIA. (APOSTD/2019/122) GENERALITAT VALENCIANA (2019-2021).

References

1. European Bioplastics. Market data about global production capacity of bioplastics on 2019. [Onoine], Available: https://www.european-bioplastics.org/market/ (accessed Feb 19, 2020).
2. Muthuraj, R.; Misra, M.; Mohanty, A. K. *J. Appl. Polym. Sci.* **2018**, 135, 45726.
3. Koller, M.; Maršálek, L.; de Sousa Dias, M. M.; Braunegg, G. *N. Biotechnol.* **2017**, 37, 24.
4. Siracusa, V.; Lotti, N.; Munari, A.; Dalla Rosa, M. *Polym. Degrad. Stab.* **2015**, 119, 35.
5. Gumede, T. P.; Luyt, A. S.; Müller, A. J. *Express Polym. Lett.* **2018**, 12, 505.
6. Garcia-Garcia, D.; Lopez-Martinez, J.; Balart, R.; Strömberg, E.; Moriana, R. *Eur. Polym. J.* **2018**, 104, 10.
7. Garcia-Garcia, D.; Garcia-Sanoguera, D.; Fombuena, V.; Lopez-Martinez, J.; Balart, R. *Appl. Clay Sci.* **2018**, 162, 487.
8. Garcia-Garcia, D.; Ferri, J. M.; Boronat, T.; Lopez-Martinez, J.; Balart, R. *Polym. Bull.* **2016**, 73, 3333.
9. Arrieta, M. P.; Castro-López, M. D. M.; Rayón, E.; Barral-Losada, L. F.; López-Vilariño, J. M.; López, J.; González-Rodríguez, M. V. *J. Agric. Food Chem.* **2014**, 62, 10170.
10. Jamshidian, M.; Tehrany, E. A.; Imran, M.; Jacquot, M.; Desobry, S. *Compr. Rev. Food Sci. Food Saf.* **2010**, 9, 552.
11. Lim, L.-T.; Auras, R.; Rubino, M. *Prog. Polym. Sci.* **2008**, 33, 820.
12. Serna C., L.; Rodríguez de S., A.; Albán A., F. *Rev. Ing. y Compet.* **2011**, 5, 16.
13. Arrieta, M. P.; López, J.; Ferrándiz, S.; Peltzer, M. A. *Polym. Test.* **2013**, 32, 760.
14. Liu, M.; Zeng, G.; Wang, K.; Wan, Q.; Tao, L.; Zhang, X.; Wei, Y. *Nanoscale* **2016**, 8, 16819.
15. Urquijo, J.; Guerrica-Echevarría, G.; Eguiazábal, J. I. *J. Appl. Polym. Sci.* **2015**, 132, 1.
16. Tripathi, N.; Katiyar, V. *J. Appl. Polym. Sci.* **2016**, 133, 1.
17. Huang, Q.; Liu, M.; Mao, L.; Xu, D.; Zeng, G.; Huang, H.; Jiang, R.; Deng, F.; Zhang, X.; Wei, Y. *J. Colloid Interface Sci.* **2017**, 499, 170.
18. Huang, Q.; Liu, M.; Chen, J.; Wan, Q.; Tian, J.; Huang, L.; Jiang, R.; Wen, Y.; Zhang, X.; Wei, Y. *Appl. Surf. Sci.* **2017**, 419, 35.
19. Huang, H.; Liu, M.; Xu, D.; Mao, L.; Huang, Q.; Deng, F.; Tian, J.; Wen, Y.; Zhang, X.; Wei, Y. *Mater. Sci. Eng. C* **2020**, 106, 110157.
20. Pawlak, F.; Aldas, M.; López-Martínez, J.; Samper, M. D. *Polymers (Basel).* **2019**, 11, 1514.
21. Yang, S. lin; Wu, Z. H.; Yang, W.; Yang, M. B. *Polym. Test.* **2008**, 27, 957.
22. Ferri, J. M.; Garcia-Garcia, D.; Sánchez-Nacher, L.; Fenollar, O.; Balart, R. *Carbohydr. Polym.* **2016**, 147, 60.

23. Bhasney, S. M.; Patwa, R.; Kumar, A.; Katiyar, V. *J. Appl. Polym. Sci.* **2017**, 134, 1.
24. Moustafa, H.; El Kissi, N.; Abou-Kandil, A. I.; Abdel-Aziz, M. S.; Dufresne, A. *ACS Appl. Mater. Interfaces* **2017**, 9, 20132.
25. Niu, X.; Liu, Y.; Song, Y.; Han, J.; Pan, H. **2018**, 183, 102.
26. Pavon, C.; Aldas, M.; López-Martínez, J.; Ferrandiz, S. *Polymers (Basel).* **2020**, 12, 334.
27. Mitchell, G. R.; Biscaia, S.; Mahendra, V. S.; Mateus, A. *Adv. Mater. Phys. Chem.* **2016**, 06, 54.
28. Wiyono, B.; Tachibana, S.; Tinambunan, D. *Indones. J. For. Res.* **2006**, 3, 7.
29. Karlberg, A. T. *Kanerva's Occup. Dermatology, Second Ed.* **2012**, 1, 467.
30. El-Sayed Abdel-Raouf, M.; Mahmoud Abdul-Raheim, A.-R. *BAOJ Chem, an open access J.* **2018**, 4, 39.
31. Liu, B.; Nie, J.; He, Y. *Int. J. Adhes. Adhes.* **2016**, 66, 99.
32. Kumooka, Y. *Forensic Sci. Int.* **2008**, 176, 111.
33. Aldas, M.; Ferri, J. M.; Lopez-Martinez, J.; Samper, M. D.; Arrieta, M. P. *J. Appl. Polym. Sci.* **2019**, 137, 48236.
34. Kaavessina, M.; Distantina, S.; Chafidz, A.; Utama, A.; Anggraeni, V. M. P. *AIP Conf. Proc.* **2018**, 1931, 030006.
35. Safety data Sheet. SIGMA-ALDRICH; **2018**.
36. International Standards Organization. ISO 527-2:2012. Plastics - Determination of tensile properties - Part 2: Test conditions for moulding and extrusion plastics; **2012**.
37. International Standards Organization. ISO 1133-1:2012. Plastics - Determination of the melt mass-flow rate (MFR) and melt volume-flow rate (MVR) of thermoplastics - Part 1: Standard method; **2012**.
38. International Standards Organization. Plastics - Determination of water absorption; **2008**.
39. Torres-Giner, S.; Gimeno-Alcañiz, J. V.; Ocio, M. J.; Lagaron, J. M. *J. Appl. Polym. Sci.* **2011**, 122, 914.
40. International Standards Organization. ISO 178:2019. Plastics - Determination of flexural properties; **2019**.
41. International Standards Organization. ISO 179-1:2010. Plastics - Determination of Charpy impact properties - Part 1: Non-instrumented impact test; **2010**.
42. International Standards Organization. ISO 868:2003. Plastics and ebonite - Determination of indentation hardness by means of a durometer (Shore hardness); **2003**.
43. International Standards Organization. ISO 306:2013. Plastics -Thermoplastic materials - Determination of Vicat softening temperature (VST); **2013**.
44. International Standards Organization. ISO 75:2013. Plastics - Determination of temperature of deflection under load - Part 2: Plastics and ebonite; **2013**.
45. Turan, D.; Sirin, H.; Ozkoc, G. *J. Appl. Polym. Sci.* **2011**, 121, 1067.
46. Chieng, B. W.; Ibrahim, N. A.; Then, Y. Y.; Loo, Y. Y. *Molecules* **2014**, 19, 16024.
47. Sigma-Aldrich. Gum Rosin Safety data sheet; **2019**; pp 1–8.
48. Favre, H. A.; Powell, W. H. Nomenclature of Organic Chemistry - IUPAC Recommendations and Preferred Names; Royal Society of Chemistry, **2013**.
49. Pani, B.; Sirohi, S.; Singh, D.; Pani, B.; Sirohi, S.; Singh, D. *Am. J. Polym. Sci.* **2013**, 3, 63.
50. Siengalewicz, P.; Mulzer, J.; Rinner, U. Comprehensive Organic Synthesis: Second Edition; Elsevier, **2014**; Vol. 6; pp 355–410.

51. Siddiki, S. M. A. H.; Toyao, T.; Kon, K.; Touchy, A. S.; Shimizu, K. ichi. *J. Catal.* **2016**, 344, 741.
52. Robert J. Ouellette and J. David Rawn. *Princ. Org. Chem.* **2015**, 287.
53. Liang, Y. T.; Yang, G. P.; Liu, B.; Yan, Y. T.; Xi, Z. P.; Wang, Y. Y. *Dalt. Trans.* **2015**, 44, 13325.
54. Cabaret, T.; Boulicaud, B.; Chatet, E.; Charrier, B. *Eur. J. Wood Wood Prod.* **2018**, 76, 1453.
55. Ferri, J. M.; Garcia-Garcia, D.; Carbonell-Verdu, A.; Fenollar, O.; Balart, R. *J. Appl. Polym. Sci.* **2018**, 45751, 1.
56. Najafi, N.; Heuzey, M. C.; Carreau, P. J.; Wood-Adams, P. M. *Polym. Degrad. Stab.* **2012**, 97, 554.
57. Ferri, J. M.; Samper, M. D.; Garcí-a-Sanoguera, D.; Reig, M. J.; Fenollar, O.; Balart, R. *J. Mater. Sci.* **2016**, 51, 5356.
58. Nehra, R.; Maiti, S. N.; Jacob, J. *J. Appl. Polym. Sci.* **2018**, 135, 45644.
59. Odian, G. Principles of Polymerization; **2004**.
60. Sauer, J. A. *Polym. Eng. Sci.* **1977**, 17, 150.
61. de la Rosa-Ramirez, H.; Aldas, M.; Ferri, J. M.; Samper, M. D.; Lopez-Martinez, J. *J. Appl. Polym. Sci.* **2020**, 49346, 1.

Issn 0021-8995